Supplementary Information

Intestinal IL-25 prevents high-fat diet-induced obesity by modulating the cholesterol transporter NPC1L1 expression in the intestinal epithelial cells

Running title: The role of intestinal IL-25 during high-fat diet-induced obesity

Siranart Jeerawattanawart[1, 2], Pornpimon Angkasekwinai[1, 3*]

[1]Department of Medical Technology, Faculty of Allied Health Sciences, Thammasat University, Pathum Thani 12120 Thailand.

[2]Faculty of Medical Technology, Rangsit University, Pathum Thani 12000, Thailand.

[3]Research Unit in Molecular Pathogenesis and Immunology of Infectious Diseases, Thammasat University, Pathum Thani 12120 Thailand.

*** Correspondence:**

Pornpimon Angkasekwinai

upornpim@tu.ac.th, p.akswn@gmail.com

Supplementary Table S1. Oligonucleotide primers used for Quantitative real-time PCR.

Gene	Primer sequence (5'-3')
Mouse *Sglt1*	Forward: TCA GCC TCA GGT GGA CTT TGT G Reverse: ATC ATT GGC CAT GCA ATG AAA C
Mouse *Glut2*	Forward: ACA CCG GAA TGT TCT TAG CC Reverse: GTG AGA GAA GCC GAG GAA AG
Mouse *Glp1*	Forward: CCT TCA AGA CAC AGA GGA GAA CC Reverse: CTG TAG TCG CTG GTG AAT GTG C
Mouse *Npc1l1*	Forward: ATC GCA CTA CCA TCC AGG ACC T Reverse: CCC AGA GTA GCC TTG GAA TCC A
Mouse *Scarb1*	Forward: ACA CCC GAA TCC TCG CTG GAA T Reverse: CCG TTG GCA AAC AGA GTA TCG G
Mouse *Fatp4*	Forward: GAC TTC TCC AGC CGT TTC CAC A Reverse: CAA AGG ACA GGA TGC GGC TAT TG
Mouse *Cd36*	Forward: GGA CAT TGA GAT TCT TTT CCT CTG Reverse: GCA AAG GCA TTG GCT GGA AGA AC
Mouse *Mogat2*	Forward: CAC GGG CTT TAC CTC GCT TTT C Reverse: CCT GGA CAG AAT GTG ATC GGC A
Mouse *Apobec1*	Forward: TCA GGG ACC TTA TTA GCA GCG G Reverse: GCC AAT AAG CTT CGT TTG AAG GG
Mouse *Mttp*	Forward: ATG ATC CTC TTG GCA GTG CTT Reverse: TGA GAG GCC AGT TGT GTG AC
Mouse *Dgat1*	Forward: GGT TCC GTG TTT GCT CTG GCA T Reverse: CCA CTG ACC TTC TTC CCT GTA G
Mouse *Acat2*	Forward: GAG ATT GTG CCA GTG CTG GTG T Reverse: GTG ACA GTT CCT GTC CCA TCA G
Mouse *Tnfa*	Forward: CAG GCG GTG CCT ATG TCT C Reverse: CGA TCA CCC CGA AGT TCA GTA G
Mouse *Il25*	Forward: CAC ACT GCG TCA GCC TAC AGA Reverse: TGT CGT AAA GTG GGA CGG AGT

Mouse *Tslp*	Forward: TCG AGG ACT GTG AGA GCA AGC CAG Reverse: CTG GAG ATT GCA TGA AGG AAT ACC A
Mouse *Il33*	Forward: TCC TTG CTT GGC AGT ATC CA Reverse: TGC TCA ATG TGT CAA CAG ACG
Mouse *Dclk1*	Forward: CAA GCC AGC CAT GTC GTT C Reverse: TTC CTT TGA AGT AGC GGT CAC
Mouse *Srebp2*	Forward: AGA AAG AGC GGT GGA GTC CTT G Reverse: GAA CTG CTG GAG AAT GGT GAG G
Mouse and Human *Actb*	Forward: GAC GGC CAG GTC ATC ACT ATT G Reverse: AGG AAG GCT GGA AAA GAG CC
Human *Npc1l1*	Forward: TGC TGT TGT GCA GCC TCT CTG A Reverse: CCA CAA AGG CTG ACA TCT GCA G
Human *Scarb1*	Forward: GGT CCA GAA CAT CAG CAG GAT C Reverse: GCC ACA TTT GCC CAG AAG TTC C
Human *Cd36*	Forward: CAG GTC AAC CTA TTG GTC AAG CC Reverse: GCC TTC TCA TCA CCA ATG GTC C
Human *Fatp4*	Forward: GGA CCA ACT TTT CCA GCC GCT T Reverse: TGC GGC TAT TGA AAC CAC AGG C
Human *Abcg5*	Forward: GAT TGT CGT CCT CCT GGT GGA A Reverse: TCT CCG AAG CTC AGG ATG GCA A
Human *Abcg8*	Forward: TGT CCT CGC TAC AGC AAT CCT G Reverse: AGA AAC AGG GCT GCG AGT GAC T
Human *Abcb1*	Forward: GGC CTA ATG CCG AAC ACA TT Reverse: CAG CGT CTG GCC CTT CTT C
Human *Abca1*	Forward: CAG GCT ACT ACC TGA CCT TGG T Reverse: CTG CTC TGA GAA ACA CTG TCC TC
Human *Hnf1a*	Forward: ACC TGT CCC AAC ACC TCA AC Reverse: TGG TAG CTC ATC ACC TGT GG
Human *Hnf4a*	Forward: GGT GTC CAT ACG CAT CCT TGA C Reverse: AGC CGC TTG ATC TTC CCT GGA T

Human *Srebp2*	Forward: CTC CAT TGA CTC TGA GCC AGG A Reverse: GAA TCC GTG AGC GGT CTA CCA T
Human *Hmgcr*	Forward: GAG GTG AAC CTA TGC TGG TCA G Reverse: GGT ATC TGT TTC AGC CAC TAA GG
Human *Ldlr*	Forward: GAA TCT ACT GGT CTG ACC TGT CC Reverse: GGT CCA GTA GAT GTT GCT GTG G

Sglt1, Sodium-glucose cotransporter1; *Glut2*, Solute carrier family 2 member 2; *Glp1*, Glucagon Like Peptide 1; *Npc1l1*, Niemann-Pick C1-Like Protein 1; *Scarb1*, Scavenger Receptor Class B Member 1; *Fatp4*, Fatty acid transport protein 4; *Cd36*, Cluster of differentiation 36; *Mogat2*, Monoacylglycerol O-Acyltransferase 2; *Apobec1*, Apolipoprotein B mRNA editing enzyme catalytic subunit 1 ; *Mttp*, Microsomal triglyceride transfer protein; *Dgat1*, Diacylglycerol O-acyltransferase 1; *Acat2*, Acetyl-CoA acetyltransferase 2; *Tnfa*, Tumor Necrosis Factor-Alpha; *Il25*, Interleukin 25; *Tslp*, Thymic Stromal Lymphopoietin; *Il33*, Interleukin 33; *Dclk1*, doublecortin-like kinase 1; *Srebp2*, sterol regulatory element binding protein 2, *Actb*, β-actin; *Abcg5*, ATP binding cassette subfamily G member 5; *Abcg8*, ATP binding cassette subfamily G member 8, *Abcb1*, ATP binding cassette subfamily B member 1; *Abca1*, ATP binding cassette subfamily A member 1, *Hnf1a*, HNF1 homeobox A; *Hnf4a*, hepatocyte nuclear factor 4 alpha; *Hmgcr*, 3-hydroxy-3-methylglutaryl-CoA reductase; *Ldlr*, low density lipoprotein receptor

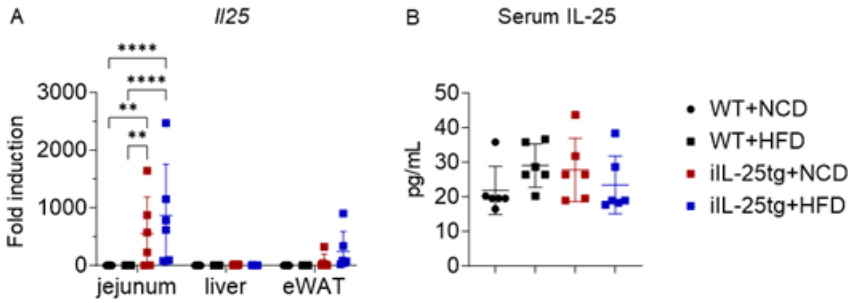

Supplementary Figure S1. Comparison of IL-25 expression in various cellular sources between littermate control and iIL-25tg mice during HFD-induced obesity. iIL-25tg or littermate control BALB/c mice were fed with NCD or HFD for 8 weeks, and the expression of IL-25 was evaluated in the jejunum, liver, eWAT, and serum. (A) Quantitative real-time PCR analysis of *Il25* in the jejunum, liver, and eWAT of iIL-25tg and littermate control mice fed either NCD or HFD. The mRNA expression data are presented as fold induction over actin (*Actb*) expression, with the mRNA levels in littermate control NCD-fed mice set as 1. (B) ELISA analysis of IL-25 in serum from littermate control and iIL-25tg mice. Graphs depict mean ± SD of three independent experiments, with n = 6 mice per group. Significance was determined using two-way ANOVA with Uncorrected Fisher's LSD, with a single pooled variance and one-way ANOVA followed by Turkey post hoc analysis (**p<0.01, ***p<0.001, ****p<0.0001).

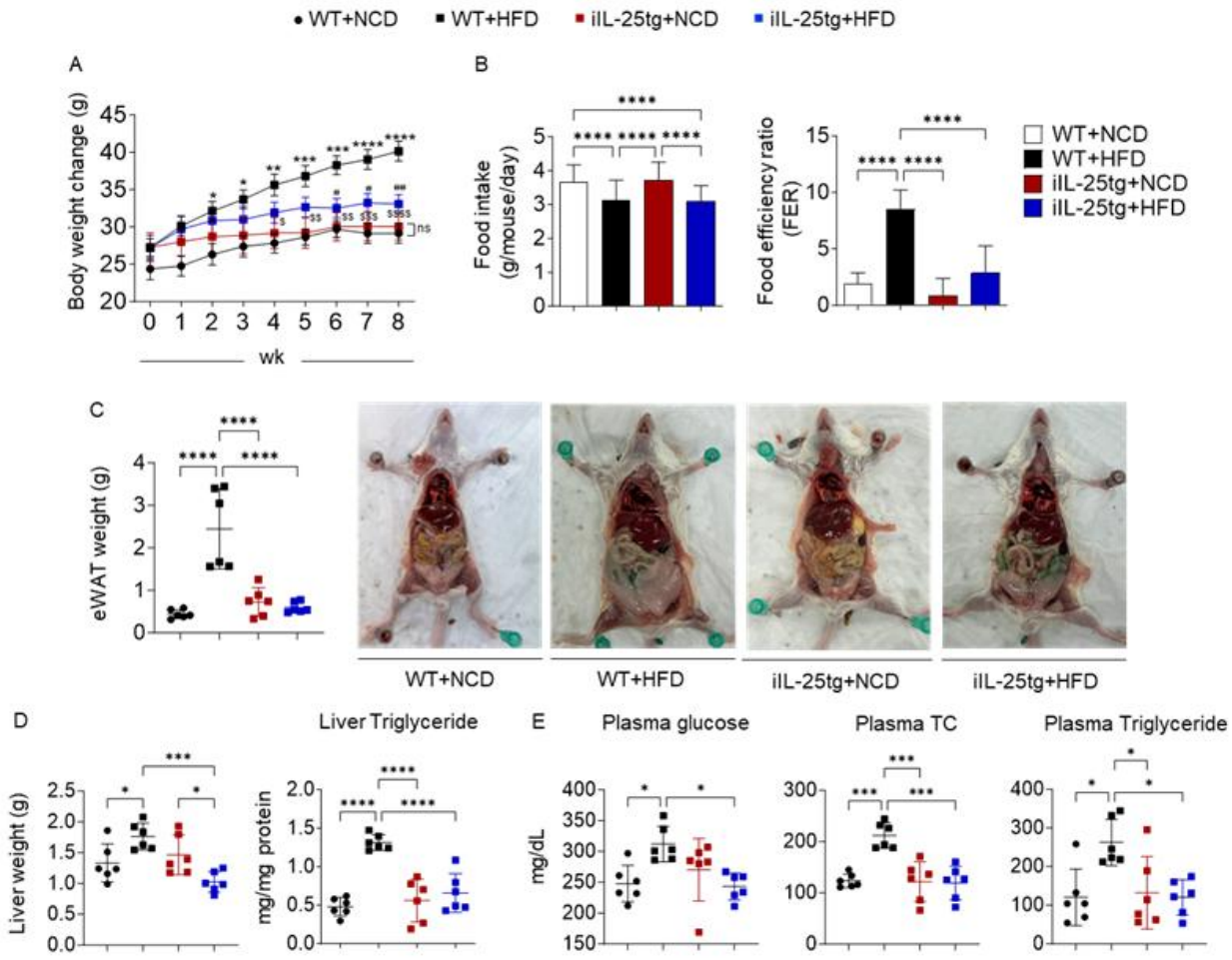

Supplementary Figure S2. The effect of HFD feeding on systemic metabolic changes in littermate control and iIL-25tg mice. iIL-25tg or littermate control BALB/c mice were fed with NCD or HFD for 8 weeks and metabolic changes were evaluated. (A) Body weight gain (g) was measured weekly between each group. (B) Food intake (g/mouse/day) and Food efficiency ratio (FER) were calculated for iIL-25tg or littermate control BALB/c mice fed with NCD or HFD by dividing body weight gain (g/day) by daily food intake (g/day), multiplied by 100. (C) eWAT weight (g) and representative picture of abdominal fat in each group after 8 weeks of feeding. (D) Liver weight (g) and the amounts of liver triglycerides (mg/mg protein) in each group after 8 weeks of feeding. (E) Plasma concentration of glucose, total cholesterol (TC), and triglyceride (mg/dL) in each group after 8 weeks of feeding. Graphs depict mean ± SD of three independent

experiments, with n = 6 mice per group. Significance was determined using two-way ANOVA with Dunnett's multiple comparisons test (Supplementary Fig. S2A) (*p<0.05, **p<0.01, ***p<0.001, ****p<0.0001; comparison between WT+NCD and WT+HFD, $$p$<0.05, $$$p$<0.01, $$$$p$<0.001, $$$$$p$<0.0001; comparison between iIL-25tg+NCD and WT+HFD, #p<0.05, ##p<0.01; comparison between iIL-25tg+HFD and WT+HFD, NS; non-significant; and one-way ANOVA followed by Turkey post hoc analysis (Supplementary Fig. S2B-E) (*p<0.05, ***p<0.001, ****p<0.0001).

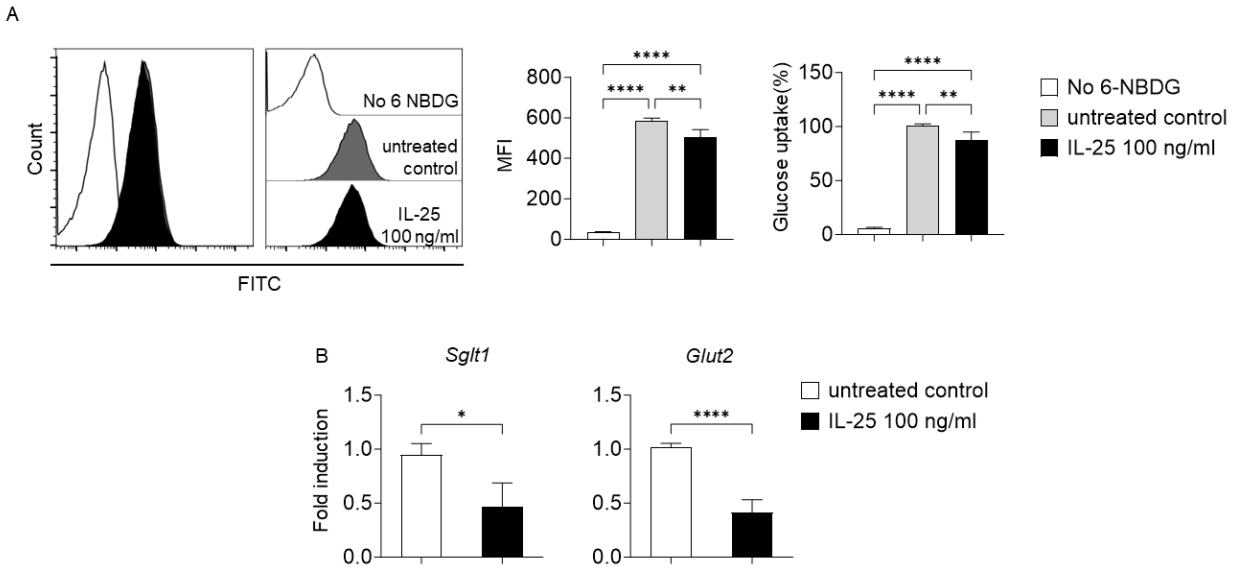

Supplementary Figure S3. The effect of IL-25 treatment on glucose uptake in Caco-2 cells. Caco-2 cells were cultured in 24-well plate for 21 days. Cells were pretreated with or without 100 ng/mL human recombinant IL-25 for 24 hours before analysis of glucose uptake using 6-NBDG and gene expression. (A) Representative histogram and graph show mean fluorescence level (MFI) and percentage (%) of glucose uptake using 6-NBDG in Caco-2 cells by flow cytometric analysis. (B) Quantitative real time PCR analysis of *Sglt1* and *Glut2* mRNA expression. Data are presented as fold induction over actin (*Actb*) expression, with the mRNA levels in the control untreated cell set as 1. Graphs depict mean ± SD of three independent experiments. Significance was determined using one-way ANOVA followed by Turkey post hoc analysis and Student's t-test (*p<0.05, **p<0.01, ***p<0.001, ****p<0.0001).

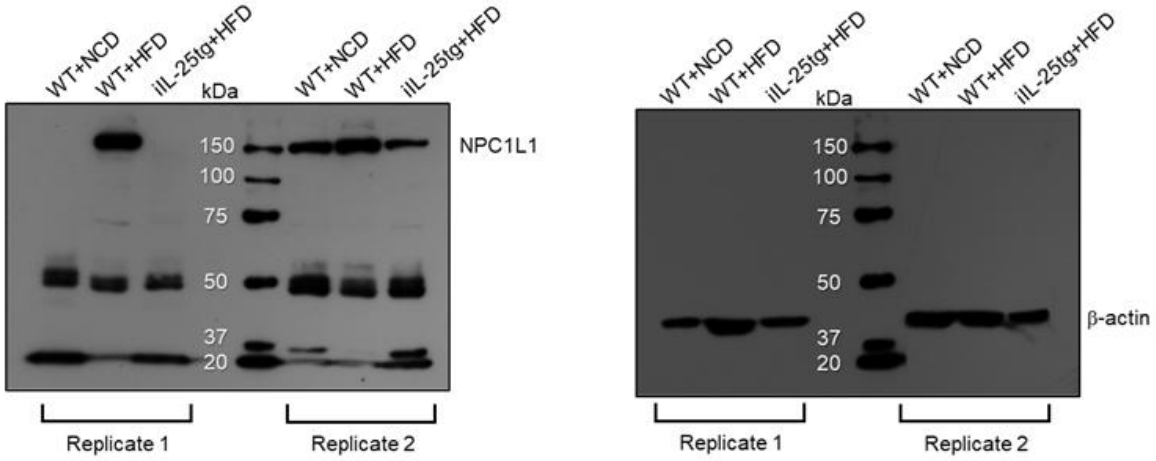

Supplementary Figure S4. Determination of NPC1L1 transporter protein expression in the intestine of littermate control or iIL-25tg mice during high-fat diet-induced obesity. Full-length blots from western blot analysis of the NPC1L1 protein expression in in the jejunum lysate of iIL-25tg or littermate control HFD-fed mice compared with littermate control NCD-fed mice. Lane M represents molecular weight protein marker (kDa). The expected molecular weights of NPC1L1and β-actin are 145 kDa, and 42 kDa, respectively. The images showed the protein expression levels of NPC1L1 from experimental replicates 1 and 2.

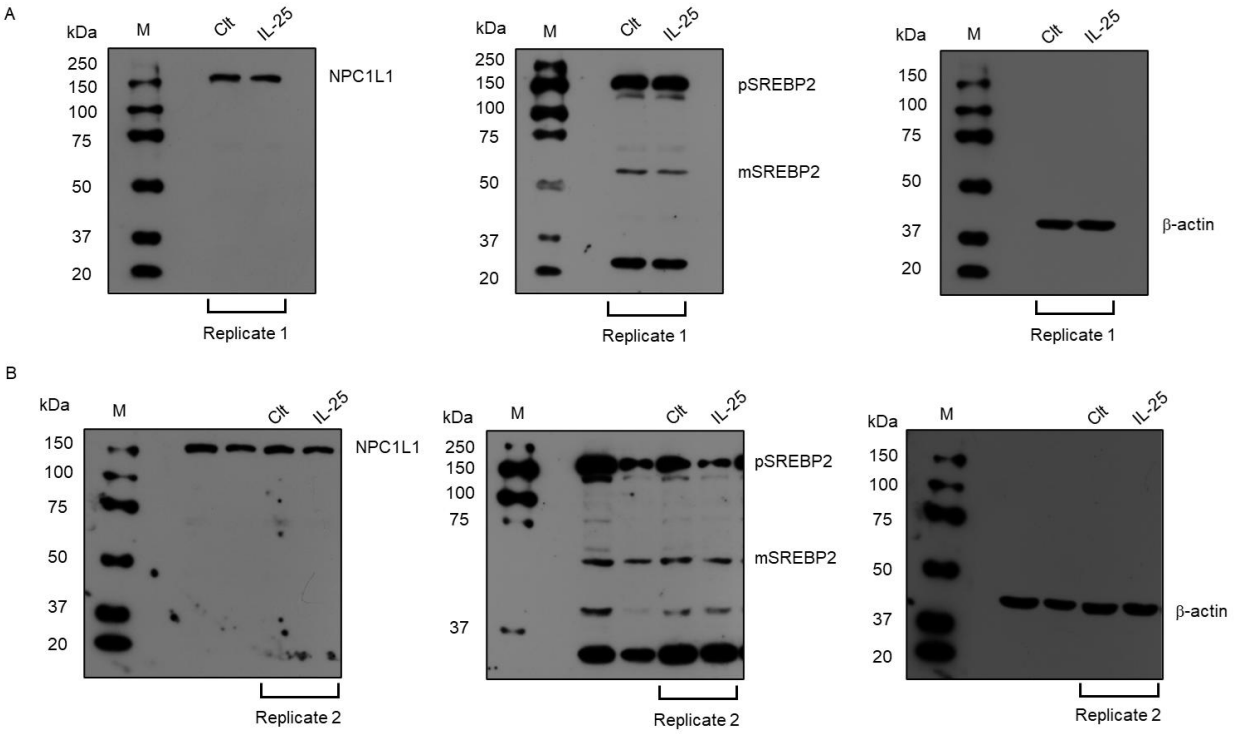

Supplementary Figure S5. The contribution of IL-25 to the protein expression of NPC1L1 and its positive transcriptional regulator SREBP2 in Caco-2 cells. Full-length blots from western blot analysis of the NPC1L1, pSREBP2, and mSREBP2 protein expression in the protein lysate of Caco-2 cells treated with or without IL-25 for 24 hours. Lane M represents molecular weight protein marker (kDa). The expected molecular weights of NPC1L1, pSREBP2, mSREBP2, and β-actin are 145 kDa, 126 kDa, 55 kDa, and 42 kDa, respectively. (A) The images showed the protein expression levels of NPC1L1, pSREBP2, and mSREBP2 from experimental replicate 1. (B) The images showed the protein expression levels of NPC1L1, pSREBP2, and mSREBP2 from experimental replicate 2.